

# Pressure Effects on the Physical Properties of Lipid Bilayers Detected by *trans*-Parinaric Acid Fluorescence Decay

C. Reyes Mateo,\*Patrick Tauc, and Jean-Claude Brochon

Laboratoire pour l'Utilisation du Rayonnement Electromagnétique, Centre National de la Recherche Scientifique-Ministère de l'Éducation Nationale-Commissariat à l'Énergie Atomique, Bâtiment 209D, Université Paris Sud, 91405 Orsay, France

**ABSTRACT** The effects of hydrostatic pressure on the physical properties of large unilamellar vesicles of single lipids dipalmitoyl phosphatidylcholine (DPPC) and dimyristoyl phosphatidylcholine (DMPC) and lipid mixtures of DMPC/DPPC have been studied from time-resolved fluorescence of *trans*-parinaric acid. Additional experiments were carried out using diphenylhexatriene to compare the results extracted from both probes. Fluorescence decays were analyzed by the maximum entropy method. Pressure does not influence the fluorescence lifetime distribution of *trans*-parinaric acid in isotropic solvents. However, in pressurized lipid bilayers an abrupt change was observed in the lifetime distribution which was associated with the isothermal pressure-induced phase transition. The pressure to temperature equivalence values,  $dT/dP$ , determined from the midpoint of the phase transitions, were 24 and 14.5°C kbar<sup>-1</sup> for DMPC and POPC, respectively. Relatively moderate pressures of about 500 bar shifted the DMPC/DPPC phase diagram 11.5°C to higher temperatures.

The effects of pressure on the structural properties of these lipid vesicles were investigated from the anisotropy decays of both probes. Order parameters for all systems increased with pressure. In the gel phase of POPC the order parameter was smaller than that obtained in the same phase of saturated phospholipids, suggesting that an efficient packing of the POPC hydrocarbon chains is hindered.

## INTRODUCTION

The study of the physical properties of lipid bilayers is of fundamental importance in membrane research because these bilayers constitute the fundamental matrix of biological membranes and represent the environment where many proteins display their activity. Concretely, there are three properties of the lipid bilayer which are of particular relevance for the diversity of membrane functions: orientational order, fluidity, and lateral heterogeneity. Fluidity and orientational order are, respectively, related to the rate and extent of phospholipid acyl chain motions away from an average orientation. Lateral heterogeneity results from the lack of miscibility of some bilayer components which form "domains" with specific physical properties.

At constant pressure, the more frequently perturbing variables used to study the structural properties of a biological system are chemical composition and temperature. The changes induced in the physical properties of the membrane upon chemical composition modifications are linked to every specific type of lipid. Temperature changes result in simultaneous alterations of the thermal energy and volume, making it very difficult to distinguish between the effects due to the thermally activated process (rotational diffusion, thermodynamics friction, etc.) and those related to the change of the density and packing of the system. Pressure changes at constant temperature introduce large changes in those parameters which depend exclusively upon the volume.

The effects of hydrostatic pressure on lipid bilayers and cellular membranes have been studied by fluorescence probe techniques (Chong et al., 1983a; Chong and Weber, 1983b; Chong, 1988; Behan et al., 1992; Sassaroli et al., 1993) as well as other physical techniques including NMR spectroscopy (Jonas et al., 1988; Peng and Jonas, 1992), ESR (Trudell et al., 1974), neutron diffraction (Braganza and Worcester, 1986a; Braganza and Worcester, 1986b), light scattering (Ceuterick et al., 1978), and volumetry (Liu and Kay, 1977; Tosh and Collings, 1986). From an experimental point of view, time-resolved fluorescence probe spectroscopy allows the study of the pressure-induced membrane structural changes, at a molecular level, in a simple way. The success of the method depends on the interpretation of the changes observed in the photophysical parameters of the probes.

Pressure can alterate the location of the probe in the lipid bilayer and, consequently, complicate the interpretation of data. The use of fluorescent fatty acids and lipid derivatives may overcome this problem to a considerable extent. In our previous study (Mateo et al., 1993a), it was shown that the fluorescent fatty acid *trans*-parinaric acid (*t*-PnA) can be used to detect and quantify gel-fluid heterogeneity in lipid bilayers. In the present work, the photophysical parameters (lifetimes, fluorescence anisotropy, and excitation/emission spectra) of this probe have been used to investigate the effects of hydrostatic pressure (1 bar to 3 kbar) on the physical properties of lipid bilayers. The influence of composition of pure as well as mixtures of phospholipids have been studied. In addition, some of the experiments have been carried out using 1,6-diphenyl-1,3,5-hexatriene (DPH) as a fluorescent probe in order to compare the information extracted from both probes. The results show that the isotherm pressure-induced phase transition can be detected with high precision

Received for publication 4 June 1993 and in final form 5 August 1993.

Address reprint requests to Dr. J. C. Brochon.

\*Present address: Instituto de Química Física, CSIC, Serrano 119, 28006 Madrid, Spain.

© 1993 by the Biophysical Society

0006-3495/93/11/2248/13 \$2.00

from the changes observed in the lifetime distribution of *t*-PnA. The lifetime distributions of DPH are slightly sensitive to these phase transitions. The effects of pressure on the physical properties of the bilayers have been quantified from the time-resolved fluorescence anisotropy decays of both probes. Order parameters and "microviscosities" increased with pressure in all the systems. The effects of pressure on the phase diagram of lipid mixtures are also discussed.

## MATERIALS AND SAMPLE PREPARATION

DPH, obtained from Sigma Chemical Co. (St. Louis, MO) was recrystallized from hexane. *t*-PnA was obtained from Molecular Probes, Inc. (Eugene, OR) and used without additional purification. Purity was checked by both absorption and emission spectroscopy and high-performance liquid chromatography. Dipalmitoyl phosphatidylcholine (DPPC) and dimyristoyl phosphatidylcholine (DMPC) were obtained from Serdary (London, Ontario, Canada) and palmitoyloleoyl phosphatidylcholine (POPC) from Sigma. These chemicals were used as supplied. Stock solutions of DPH and *t*-PnA were prepared in dimethylformamide and ethanol, respectively, and stored in the dark at  $-20^{\circ}\text{C}$  before use. The stock solution was vigorously bubbled with nitrogen before the tube was capped.

Large unilamellar vesicles (LUV), with a mean diameter of 90 nm, were prepared from the multilamellar vesicles by extrusion techniques (Hope et al., 1985) through Nucleopore filters with 100-nm pore size. The probe was added as aliquots from the stock solution directly into the lipidic dispersion, as described in the preceding paper (Mateo et al., 1993a). The probe/lipid molar ratio was 1/200 for *t*-PnA and 1/500 for DPH. Samples were used immediately after preparation.

## FLUORESCENCE MEASUREMENTS

Time-resolved fluorescence and fluorescence anisotropy decays under pressure were recorded with a high-pressure optical cell mounted in a time-correlated single photon counting fluorimeter. For a strict comparison, the fluorescence decays at atmospheric pressure were also carried out using this pressure optical cell. The high pressure system, including the optical cell, inner cuvette, and pressure-generating system, were similar to those described by Paladini and Weber (1981). The sample was loaded into a cylindrical quartz cuvette capped with a small polyethylene tube sealed at one end, forming a closed system. The sample system was surrounded with pure ethanol which served as the pressure-transmitting fluid. The sample was thermostated by pumping water from a thermostat through channels drilled in the steel walls of the pressure cell. The anisotropy decay  $r(t)$  was extracted from the parallel  $I_{vv}(t)$  and perpendicular  $I_{vh}(t)$  polarized fluorescence decay components elicited by vertically polarized excitation. The polarized components were collected alternately by rotating the analyzer polarizer every 40 s over 30 periods. Corrections for strain birefringence of the quartz windows of the pressure optical cell at every pressure and temperature were made. The corresponding experimental G-factor =  $I_{vv}/I_{vh}$  was determined from *t*-PnA in ethanol and from DPH in cyclohexane at the same conditions. Total fluorescence intensity,  $I(t)$ , was recorded by orientating the emission polarizer at the "magic" angle of  $54.75^{\circ}$  or by summing the parallel and twice the corrected perpendicular components. For *t*-PnA fluorescence, the excitation

light pulse source was a picosecond laser system (Spectra-Physics) including a pumping Argon-Ion laser (SP 2030), a cavity dumped and synchronously dye laser (SP 375) providing a light pulse of 10–15 ps at 600 nm and at 300 nm through a frequency doubler (SP 390). The repetition rate of the excitation was set at 800 kHz. The excitation wavelength was at 300 nm and the fluorescence selected through a monochromator (Jobin-Yvon H 10; S. A. Instruments, Longjumeau, France) set at 405 nm ( $\Delta\lambda = 6$  nm) was achieved by means of a microchannel plate photomultiplier (Hamamatsu R1564U-06; Hamamatsu Photonics K.K., Hamamatsu City, Japan). The instrumental response function (80–100 ps) was recorded using the same sample by detecting around 300 nm the light scattered from the liposomes. The time scaling was 18, 35, and 75 ps per channel and 2048 channels were used. Further details of the picosecond lifetime apparatus have been published (Moya et al., 1986). In the case of DPH the samples were excited using the synchrotron radiation emitted by the positron storage ring of Orsay working at a frequency of 8.33 MHz in the two-bunch mode. The storage ring provides a light pulse with a full width at half maximum (FWHM) of  $\approx 500$  ps. Vertically polarized excitation was set to 360 ( $\Delta\lambda = 1$  nm). The emission was selected at 430 ( $\Delta\lambda = 4$  nm) and was detected by a Hamamatsu microchannel plate R1564U-06. The apparatus response function was measured, in alternation with the parallel and perpendicular components of the polarized fluorescence decay, with a scattering ludox solution near the emission wavelength. Time resolution was 31 ps per channel, and 2048 channels were used for decay storage.

## ANALYSIS AND INTERPRETATION OF DATA

Analysis of the total fluorescence intensity  $I(t)$  and of the fluorescence anisotropy  $r(t)$  were performed by the Maximum Entropy Method, MEM (Brochon and Livesey, 1988; Brochon et al., 1992). In the analysis of  $r(t)$ , all the emitting species were assumed to display the same intrinsic anisotropy and rotational dynamics. The parallel  $I_{vv}(t)$  and perpendicular  $I_{vh}(t)$  components of the fluorescence intensity at time  $t$  after the start of the excitation are:

$$I_{vv}(t) = \frac{1}{3} E_{\lambda}(t) * \left[ \int_0^{\infty} \alpha(\tau) e^{-t/\tau} d\tau \left( 1 + 2 \int_0^{\infty} \rho(\theta) e^{-t/\theta} d\theta \right) \right] \quad (1)$$

$$I_{vh}(t) = \frac{1}{3} E_{\lambda}(t) * \left[ \int_0^{\infty} \alpha(\tau) e^{-t/\tau} d\tau \left( 1 - \int_0^{\infty} \rho(\theta) e^{-t/\theta} d\theta \right) \right] \quad (3a)$$

and

$$r_0 = \int_0^{\infty} \rho(\theta) d\theta, \quad (3b)$$

where  $E_{\lambda}(t)$  is the temporal shape of the excitation flash,

\* denotes a convolution product, and  $\alpha(\tau)$  and  $\rho(\theta)$  are, respectively, the distribution functions of the fluorescence lifetimes and the rotational correlation times. The  $\alpha(\tau)$  profile is given from the initial analysis of the total fluorescence intensity  $I(t)$  by MEM and is held constant in a subsequent analysis of  $I_{vv}(t)$  and  $I_{vh}(t)$  which provides the distribution  $\rho(\theta)$  of correlation times (Brochon et al., 1992). 100 lifetime values, ranging from 0.1 to 100 ns and equally spaced on the logarithmic scale, were used for the analysis of  $\alpha(\tau)$ . The analysis of  $\rho(\theta)$  was performed starting with 100 correlation times ranging from 0.1 to 50 ns.

The anisotropy decay of *t*-PnA in lipid systems where different environments coexist was fit by the "associated" model detailed in the preceding article. In this model  $r(t)$  is approximated by assuming two probe populations, S and F, which are characterized by specific fluorescence decay,  $I_S(t)$  and  $I_F(t)$ , respectively, and anisotropy decay,  $r_S(t)$  and  $r_F(t)$ , respectively. The fluorescence decay for each probe population is described by a sum of exponentials. The respective anisotropy decay is defined by a single rotational correlation time  $\theta$  plus a residual anisotropy  $r_\infty$ . The total anisotropy decay is the linear combina-

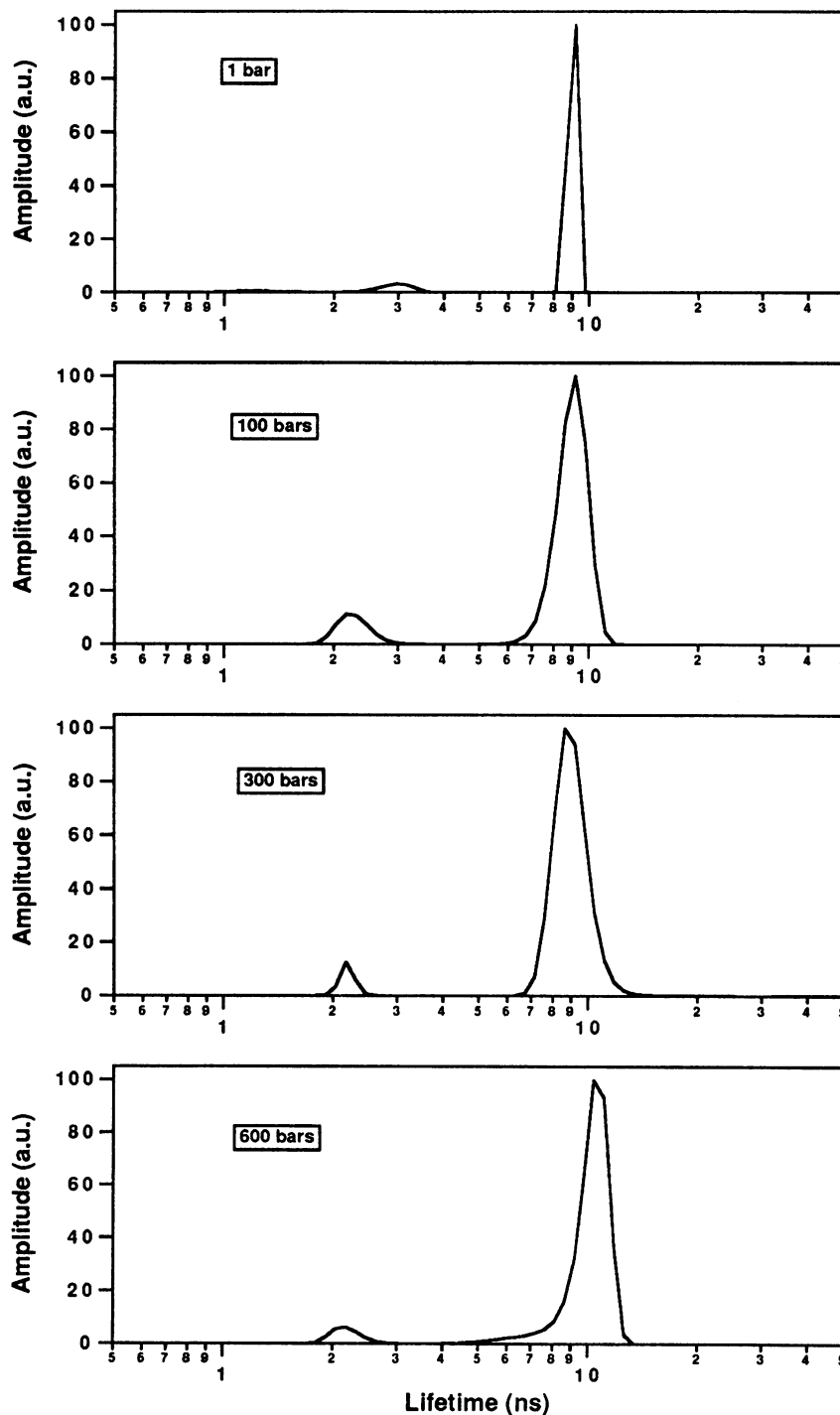


FIGURE 1 Effect of pressure on the fluorescence lifetime distribution of DPH in DMPC large unilamellar vesicles at 35°C.

tion of the anisotropy decays of the two populations of the probe:

$$r(t) = f_S(t)r_S(t) + f_F(t)r_F(t), \quad (4)$$

where  $f_S(t) = a_S I_S(t)/(a_S I_S(t) + a_F I_F(t))$  and  $f_F(t) = a_F I_F(t)/(a_S I_S(t) + a_F I_F(t))$  are the time-resolved fraction of the total fluorescence  $I(t)$  contributed by the probe population localized in the gel (S) and fluid (F) environment, respectively.

The fraction of gel phase in the bilayer can be quantified from the expression:

$$K_p^{S/F} = \frac{\chi_p^S/\chi_p^S}{\chi_p^F/\chi_p^F} \quad (\chi^S + \chi^F = 1), \quad (5)$$

where  $K_p^{S/F}$  is the partition coefficient of the probe between the gel and fluid phases and  $\chi_p^S$  and  $\chi_p^F$  are the fraction of probe localized in each phase, respectively. These fractions can be estimated from the amplitudes of the total fluorescence decay (see preceding paper (Mateo et al., 1993a)) if the radiative rate constants and extinction coefficients of the probe are similar in both phases.

The second rank order parameter  $\langle P_2 \rangle$  of a fluorescent probe with cylindrical symmetry (emission and transition moments assumed parallel) is related to the residual anisotropy  $r_\infty$  by (Jähnig et al., 1979):

$$\langle P_2 \rangle = \left( \frac{r_\infty}{r_0} \right)^{1/2}. \quad (6)$$

Values of  $r_0 = 0.385$  (Ameloot et al., 1984; Best et al., 1987) and  $r_0 = 0.390$  (Hudson and Cavalier, 1988) were used in this work for DPH and *t*-PnA, respectively.

Rotational diffusion coefficients of the probes in the lipid bilayer,  $D_w$ , were determined from the experimental correlation times  $\theta$  using the approximation of Kinoshita et al. (1977) based on the Brownian diffusion of the probe in a cone:

$$D_w = \frac{\sigma}{\langle \theta \rangle}, \quad (7)$$

where the numerical values of  $\sigma$  are function of  $r_\infty/r_0$  and are described in Kinoshita et al. (1984).  $\langle \theta \rangle$  is the average correlation determined from the area of the anisotropy decay curve (Kinoshita et al., 1984; Heyn et al., 1989). The coefficient  $D_w$  can also be estimated from the initial slope of the normalized  $r(t)$ , in a model-independent analysis (Ameloot et al., 1984), however, in the case of membrane suspensions, scattering artifacts may turn this approach less reliable.

For DPH,  $D_w$  may be converted to the "viscosity in the cone" or "microviscosity,"  $\eta$  (Kinoshita et al., 1984), which represents the dynamic friction against the wobbling motion by assuming Einstein's relation:

$$D_w = \frac{kT}{6\eta V_{ef}}, \quad (8)$$

where  $V_{ef}$  determines an "effective" volume of the probe

taken from measurements in paraffin oils with an average value of  $1.6 \cdot 10^{-22} \text{ cm}^3$  (Heyn et al., 1989; Mateo et al., 1993b).

## RESULTS

### Pressure effect on DMPC as detected by DPH fluorescence

The pressure dependence of the fluorescence kinetics of DPH was first studied in cyclohexane at 35°C. At atmospheric pressure MEM analysis of data showed a main lifetime component centered at 7.7 ns and a short lifetime of about 2 ns having a contribution lower than 2%. The only effect of increasing pressure, up to 600 bar, was a small change in the long lifetime from 7.7 to 7.2 ns (data not shown) which could be related to the increases of the polarizability of cyclohexane (Jones and Cunadall, 1986). Measurements above 600 bar cannot be performed due to the cyclohexane freezing.

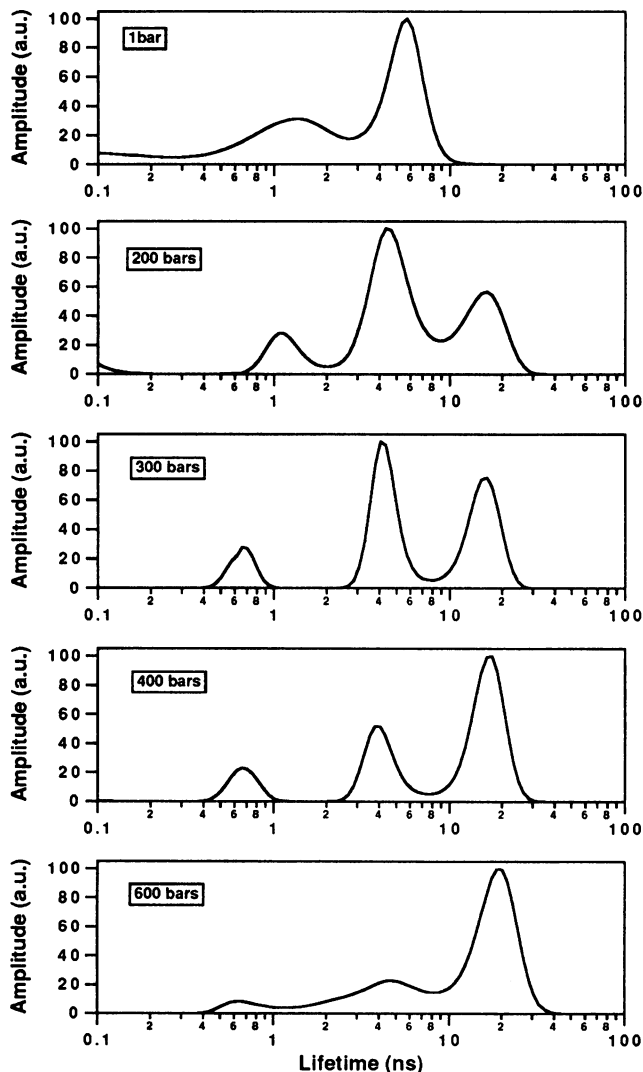


FIGURE 2 Effect of pressure on the lifetime distribution of *t*-PnA in DMPC large unilamellar vesicles at 30°C.

The effect of pressure on LUVs of DMPC was observed from the fluorescence kinetics of DPH. At 35°C and atmospheric pressure the fluorescence decay of DPH is described by a bimodal lifetime distribution, which is similar to that determined in cyclohexane. This distribution pattern is preserved up to 1000 bar (Fig. 1). The only difference is a shift of the long lifetime from 8.7 to 10.0 ns as the pressure was increased from 1 to 600 bar. No other changes were observed from 600 to 1000 bar.

### Pressure effects on DMPC, POPC, and DMPC/DPPC mixtures as detected by *t*-PnA fluorescence

The effect of hydrostatic pressure on the fluorescence kinetics of *t*-PnA was investigated in ethanol at 10°C. Analysis of data showed a bimodal fluorescence distribution at all pressures studied, up to 2000 bar, which is identical to that observed at atmospheric pressure (Mateo et al., 1993a).

The fluorescence decay of *t*-PnA in LUV of DMPC was measured isothermally as a function of pressure, up to 3000 bar, at 30° and 35°C. The results are shown in Fig. 2 and Table 1. At atmospheric pressure, the fluorescence kinetics is described by a bimodal lifetime distribution at both temperatures. At 30°C, a pressure increase of 200 bar results in the appearance of a third lifetime component centered at 15 ns. At 35°C the third component appears at pressures around 400 bar. The relative contribution of this long lifetime was found to increase as the pressure increased. This change in

**TABLE 2** Phase transition pressure,  $P_T$ , in DMPC and POPC as determined by the fluorescence kinetics of *t*-PnA and the steady-state fluorescence of perylene, DPH and dipyrnylphosphatidylcholine (dipy<sub>10</sub>PC<sup>‡</sup>)

System	<i>T</i> °C	$P_T$			
		<i>t</i> -PnA	DPH*	Perylene*	dipy <sub>10</sub> PC <sup>‡</sup>
DMPC	30	330 ± 20	310	380	300
	35	530 ± 20	510	590	480
POPC	10	1050 ± 10			800
	20	1700 ± 10			1300

\* Data from Chong et al. (1985).

‡ Data from Sassaroli et al. (1993).

the lifetime distribution pattern describes clearly the pressure-induced phase transition in DMPC. The emission spectrum of the probe does not change with pressure. The excitation spectrum shifts 3 nm to higher wavelength on increasing the pressure from 1 to 2000 bar (data not shown).

*t*-PnA accumulates in the gel phase with a partition coefficient  $K_p^{S/F} = 5 \pm 2$  (Hudson et al., 1986). Assuming that this value is preserved at high pressures, the gel phase fraction ( $\chi^S$ ) of DMPC was calculated at each pressure from the amplitude of the longest lifetime component (Table 1), as is described in the preceding paper (Mateo et al., 1993a). The correction for the measured shift in excitation spectrum upon pressure increase was taken into account. For each isothermal curve, an abrupt change was observed in  $\chi^S$

**TABLE 1** Fluorescence intensity decay parameters recovered by MEM of *t*-PnA in large unilamellar vesicles of DMPC and DMPC/DPPC (1/1) as a function of pressure

System	<i>T</i> °C	<i>P</i> bar	$C_1$	$\tau_1$ ns	$C_2$	$\tau_2$ ns	$C_3$	$\tau_3$ ns	$\chi^S$
DMPC	30.0	1	0.38	1.3	0.62	5.5			0.00
		220	0.13	1.2	0.55	4.6	0.32	15	0.14
		300	0.12	0.7	0.46	4.4	0.42	16	0.24
		400	0.10	0.7	0.28	4.2	0.62	17	0.71
		600	0.05	0.7	0.26	4.2	0.69	18	1.00
		3000	0.09	0.6	0.15	3.5	0.66	21	1.00
	35.0	1	0.18	1.0	0.82	4.2			0.00
		300	0.29	2.0	0.68	4.7	0.03	17	0.01
		500	0.21	1.4	0.24	6.3	0.55	17	0.38
		600	0.14	1.4	0.14	5.1	0.72	17	1.00
		1000	0.16	1.3	0.09	4.8	0.75	18	1.00
		DMPC/DPPC	38.0	1	0.27	0.9	0.71	4.7	0.02
100	0.27	1.2		0.63	4.9	0.10	23	0.03	
150	0.27	0.6		0.50	4.7	0.23	25	0.09	
200	0.24	1.3		0.39	5.0	0.37	25	0.20	
400	0.20	1.1		0.22	5.9	0.58	25	0.62	
500	0.16	1.0		0.16	4.7	0.68	25	1.00	
900	0.13	1.0		0.21	4.5	0.66	29	1.00	
29.0	500	0.12		1.6	0.13	5.9	0.75	34	1.00
38.5	500	0.15		1.0	0.16	4.7	0.69	25	1.00
40.0	500	0.15		1.3	0.14	6.0	0.71	24	1.00
43.0	500	0.13		0.9	0.21	4.9	0.66	22	0.76
45.0	500	0.12		1.2	0.31	4.1	0.57	21	0.46
46.0	500	0.32		1.8	0.35	5.2	0.33	21	0.15
47.7	500	0.21		1.1	0.68	3.9	0.11	21	0.04
51.5	500	0.29		1.1	0.71	3.1			0.00

$C_i$  and  $\tau_i$  are the integrated relative amplitude and center value, respectively, of each lifetime component.  $\chi^S$  is the fraction of gel phase determined from  $C_3$  (see text).  $C_i$ ,  $\pm 0.04$ ;  $\tau_1$ ,  $\pm 0.3$ ;  $\tau_2$ ,  $\pm 0.8$ ;  $\tau_3$ ,  $\pm 2$  ns.

during the pressure-induced phase transition. The phase transition pressure,  $P_T$ , can be defined as the pressure at which  $\chi^S = 0.5$ . This transition pressure was determined at each temperature and is compared in Table 2 with the values obtained in multilamellar vesicles of DMPC from perylene and DPH (Chong et al., 1985) and from dipyrnylphosphatidylcholine, dipy<sub>10</sub>PC (Sassaroli et al., 1993). The extrapolation at  $P = 1$  bar of the slope of variation of  $P_T$  versus  $T$  was  $22 \pm 2^\circ\text{C}$ , which is close to the transition temperature of DMPC,  $T_m = 23^\circ\text{C}$ . This slope gives a temperature-to-pressure equivalence  $dT/dP = 24.0 \pm 2.0^\circ\text{C kbar}^{-1}$ , which is in agreement to the value determined by other methods (Chong, 1988; Sassaroli et al., 1993; Chong et al., 1985; Macdonald et al., 1983).

The effects of pressure in LUV of POPC were studied from the fluorescence decay of *t*-PnA at  $10^\circ$  and  $20^\circ\text{C}$ . The results are shown in Fig. 3 and Table 3. At atmospheric pressure the lifetime distribution shows three components. The origin of the intermediate lifetime component is discussed in the preceding paper as a consequence of the temperature and order dependence of the *t*-PnA lifetimes. For each temperature, an abrupt change was observed in this lifetime distribution which was associated with the pressure-induced phase transition. At  $10^\circ\text{C}$ , the fluorescence distribution pattern changed sharply between 700 and 1000 bar. At  $20^\circ\text{C}$ , the changes were observed between 1300 and 1600 bar. The pressure dependence of these lifetime distributions was completely reversible.

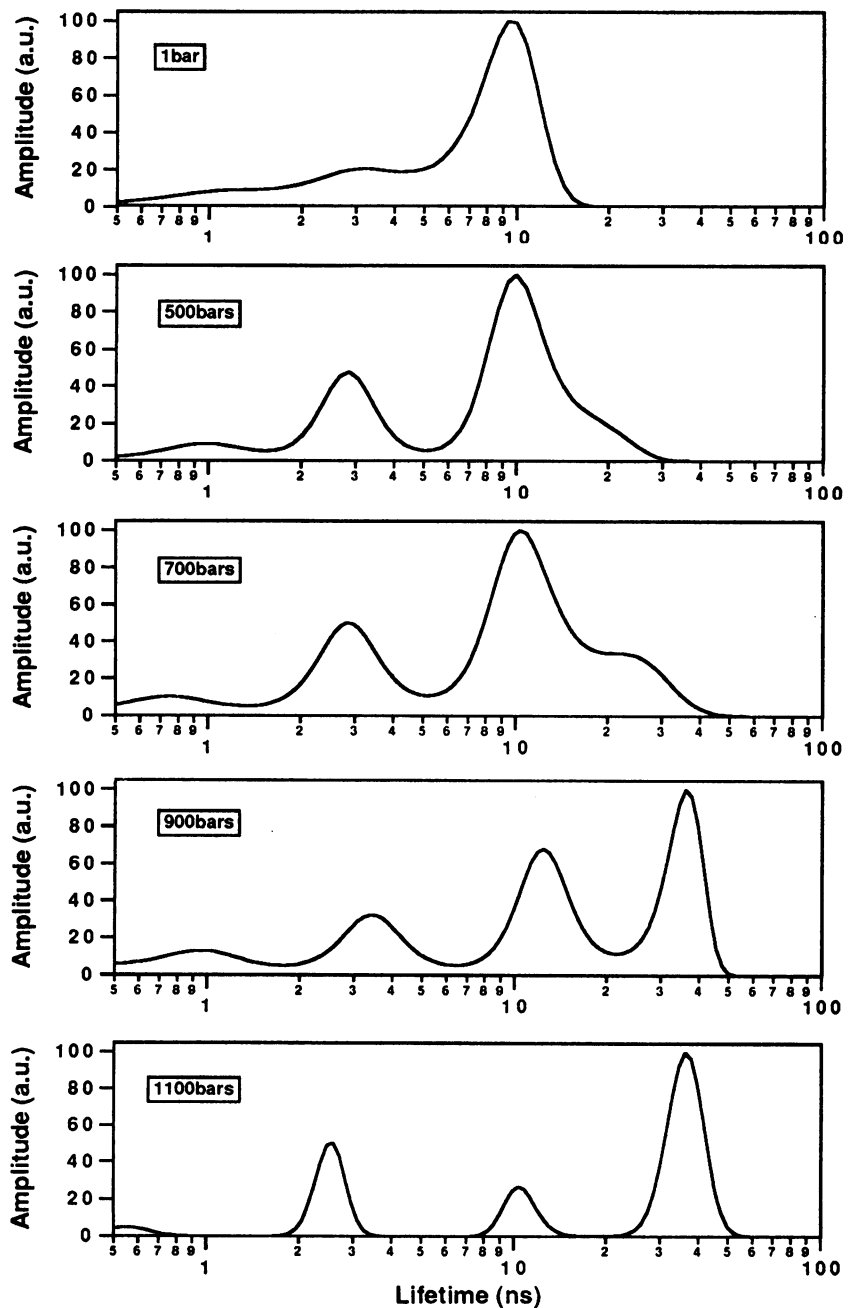


FIGURE 3 Effect of pressure on the lifetime distribution of *t*-PnA in POPC large unilamellar vesicles at  $10^\circ\text{C}$ .

**TABLE 3** Fluorescence intensity decay parameters recovered by MEM of *t*-PnA in large unilamellar vesicles of POPC as a function of pressure

System	<i>T</i>	<i>P</i>	<i>C<sub>i</sub></i>	$\tau_1$	<i>C<sub>2</sub></i>	$\tau_2$	<i>C<sub>3</sub></i>	$\tau_3$	<i>C<sub>4</sub></i>	$\tau_4$		
	°C	bars		ns		ns		ns		ns		
POPC	10	1	0.10	1.0	0.20	3.0	0.70	9.0				
		500	0.07	0.9	0.26	2.8	0.67	9.1				
		700	0.07	0.8	0.25	2.9	0.51	10.3	0.17	24		
		800	0.14	1.1	0.23	3.8	0.38	12.2	0.25	32		
		900	0.11	1.0	0.19	3.5	0.35	12.6	0.35	34		
		1100	0.04	0.5	0.24	2.5	0.14	11.0	0.58	36		
		1400	0.18	1.4	0.19	5.6			0.63	37		
		2000	0.12	1.0	0.21	4.6			0.67	40		
		POPC	20	1	0.24	0.8	0.21	1.9	0.55	6.1		
				500	0.14	0.9	0.19	2.8	0.67	8.0		
1100	0.15			0.6	0.21	2.3	0.61	8.3	0.03	26		
1300	0.11			0.9	0.27	2.6	0.49	9.1	0.13	26		
1500	0.15			0.9	0.22	3.0	0.31	9.8	0.32	26		
1600	0.09			0.6	0.24	2.6	0.25	11.0	0.42	28		
1800	0.13			0.9	0.21	4.7			0.66	25		
2100	0.12			0.8	0.13	3.3			0.75	26		

$C_i$  and  $\tau_i$  are, respectively, the integrated relative amplitude and barycenter value of each lifetime class.  $C_i$ ,  $\pm 0.04$ ;  $\tau_1$ ,  $\pm 0.2$ ;  $\tau_2$ ,  $\pm 0.8$ ;  $\tau_3$ ,  $\pm 1.5$ ;  $\tau_4$ ,  $\pm 2$  ns.

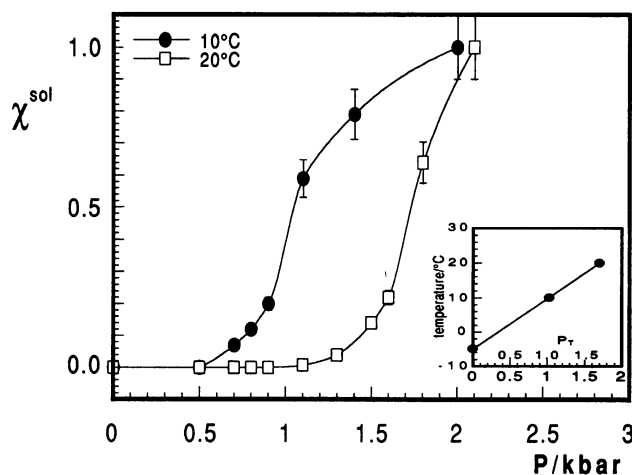


FIGURE 4 Pressure dependence of the gel fraction  $\chi^S$  of POPC at 10°C (●) and 20°C (□). Inset: phase transition pressure  $P_T$  as a function of temperature.

The partition coefficient of the probe,  $K_p^{S/F} = 5 \pm 2$ , determined in saturated systems, was assumed to be the same in POPC at any pressure. Using Eq. 4, the fraction of gel phase  $\chi^S$  was obtained as a function of pressure at 10° and 20°C (Fig. 4). As in DMPC,  $P_T$  was determined at each temperature from Fig. 4 and the value is compared in Table 2 with that estimated from dipy<sub>10</sub>PC (Sassaroli et al., 1993). The extrapolation at  $P = 1$  bar of the slope of variation of  $P_T$  versus  $T$  (see inset of Fig. 4) was  $-5.0 \pm 0.5^\circ\text{C}$ . This value is in excellent agreement with the transition temperature of POPC,  $T_m = -5^\circ\text{C}$ . The slope gives a temperature-to-pressure equivalence,  $dT/dP = 14.5 \pm 0.5^\circ\text{C kbar}^{-1}$  which is clearly smaller than the value estimated for DMPC.

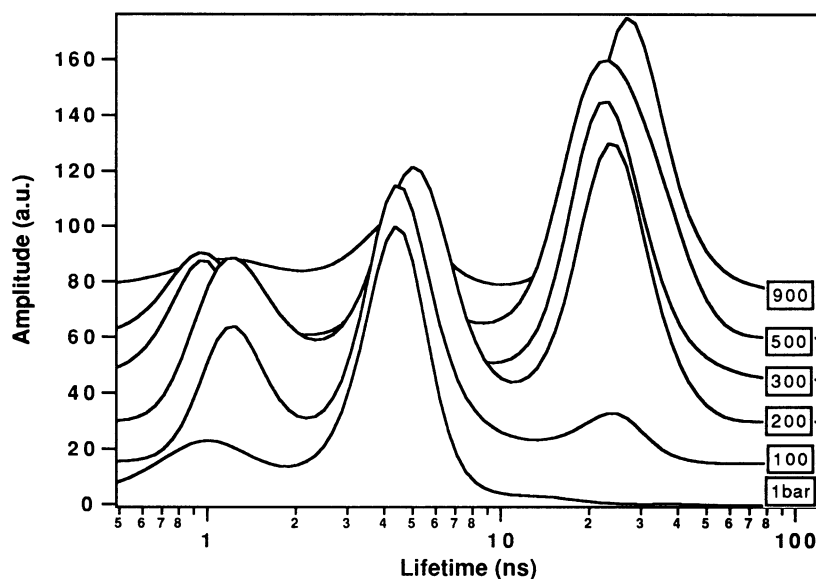
The fluorescence intensity decay of *t*-PnA was also studied in pressurized LUVs made up with an equimolar mixture of DMPC/DPPC. The selection of this specific molar proportion is supported by the experimental phase diagram which

indicates a relatively large temperature range for coexistence of both gel and fluid phases (Mateo et al., 1993a; Mabrey and Sturtevant, 1976). In addition, this temperatures range is of physiological interest. Experiments were carried out at 38.5°C in the pressure range from 1 to 900 bar and at 500 bar in the temperature range from 29° to 52°C. At atmospheric pressure and  $T = 38.5^\circ\text{C}$ , the lifetime distribution is bimodal (Fig. 5). At 100 bar this distribution is clearly modified with the appearance of a long lifetime component centered to 23 ns. The third component amplitude increases with pressure and it remains constant above 500 bar (Fig. 5 and Table 1). Fig. 6 shows the changes in the lifetime distribution induced by temperature at 500 bar. From 29° to 42°C the lifetime distribution is similar to that associated to the gel phase of a single lipid bilayer. From 43° to 47°C the contribution of the long lifetime component becomes smaller and a bimodal distribution is obtained above 48°C. The fraction of the gel phase was quantified at every temperature from the amplitude of this component and it is compared with the values obtained at atmospheric pressure (Fig. 7). The thermal phase diagram of this mixture at atmospheric pressure, previously determined from fluorescence techniques (Mateo et al., 1993a), is compared with the data obtained at 500 bar (Fig. 8). The only effect of pressure is a shift of the biphasic region of the diagram to higher temperatures. For this system a  $dT/dP = 23^\circ\text{C kbar}^{-1}$  is determined which is similar to the value obtained in DMPC.

### Pressure effects on the lipid bilayers as detected by DPH and *t*-PnA fluorescence anisotropy

Fluorescence anisotropy decay of DPH in DMPC was recorded at 35°C at several pressures. MEM analysis yielded two rotational correlation times and a residual anisotropy  $r_\infty$  (Table 4). The main effect of pressure was an increase of  $r_\infty$  which changed from 0.03 to 0.28 as pressure was increased from 1 bar to 600 bar (Fig. 9). Order parameters, diffusion

FIGURE 5 Effect of pressure on the lifetime distribution of *t*-PnA in large unilamellar vesicles of an equimolar mixture of DMPC/DPPC at 38.5°C. (For clarity, the upper curves have been vertically shifted).



coefficients and “microviscosities” were calculated from Eqs. 5–7 and are given in Table 4.

The effect of pressure on the fluorescence anisotropy decay of *t*-PnA in POPC was recorded at 10° and 20°C. The curves decay monotonically with the time to a residual anisotropy,  $r_{\infty}$ , which depends of the pressure applied (Table 5). In most of cases the curves were satisfactorily fitted assuming a single population of *t*-PnA. For the curves recorded at the transition pressures, the application of the “associated” model described in the preceding article resulted in a better fit, with a corresponding decrease in the  $\chi^2$  values from 1.14 to 1.04. This model assumes two populations of the probe which are characterized by specific lifetimes, correlation times, and order parameters. The longest lifetime component (see Fig. 3) was associated to the fraction of *t*-PnA located in the gel phase, while the short lifetime components were associated to the fraction of the probe located in the fluid phase. The results of the analysis are shown in Table 5 together with the order parameters derived from  $r_{\infty}$ . The rotational correlation times  $\theta$  display rather large uncertainty and, particularly, in the gel phase where values are close to the limit of our present experimental resolution. In most of cases, the experimental value of  $r(0)$  is lower than the theoretical value  $r_0 = 0.40$  expected for a molecule with parallel transition moments. This discrepancy can be attributed to the existence of molecular motions of the probe that are too fast to be detected under the present experimental conditions.

The anisotropy decay of *t*-PnA in an equimolar mixture of DPPC/DMPC was recorded at 38°C at several pressures (Fig. 10 and Table 5). At 500 bar the curve was described by one rotational correlation time and a high residual anisotropy. This  $r_{\infty}$  value is close to that obtained at atmospheric pressure and at temperatures below 34°C (see Table 5 in the preceding paper). At pressures lower than 500 bar anisotropy decays showed, after an initial fast decay, a subsequent gradual increase (Fig. 10). Analysis assuming a single population of probe became undoubtedly inadequate. The anisotropy

curves were satisfactorily analyzed using the “associated” exponential model. The longest lifetime component (see Fig. 5) was obviously associated to the fraction of *t*-PnA located in the more ordered lipid region, while the short lifetime components were associated to the fraction of the probe located in the fluid phase. The fit parameters are shown in Table 5 together with the order parameters. The residual anisotropies associated with the population of longer lifetime,  $r_{\infty}^S$ , do not change with pressure and are close to those obtained at 500 bar. The residual anisotropies,  $r_{\infty}^F$ , associated with the population of short lifetimes increases with pressure and are in the same range than those observed in a fluid phase at atmospheric pressure (see Table 5 in preceding paper).

## DISCUSSION

Fluorescence kinetics of *t*-PnA in lipid membranes is much more sensitive to the pressure effect than the fluorescence kinetics of DPH. The temperature-to-pressure equivalence  $dT/dP = 24.0 \pm 2.0^\circ\text{C kbar}^{-1}$ , obtained from the lifetime distributions of *t*-PnA in DMPC, is similar to that determined by other physical methods. This agreement confirms the capacity of the probe to detect with high precision the isotherm pressure-induced phase transition.

For DPH, the small change observed in the fluorescence lifetimes can be due to the increase of the lipid packing density associated to the phase transition. Given the very hydrophobic nature of the probe, this change can be also the result of a pressure induced migration of the probe into a more hydrophobic environment of the bilayer. Contrary to this, *t*-PnA remains anchored to the phospholipid polar head-groups with a rather limited migration within the bilayer. Therefore, the strong change in its fluorescence distribution can be exclusively attributed to the increase of the lipid packing density.

The changes observed in the fluorescence lifetime distribution of *t*-PnA upon the isotherm pressure-induced phase



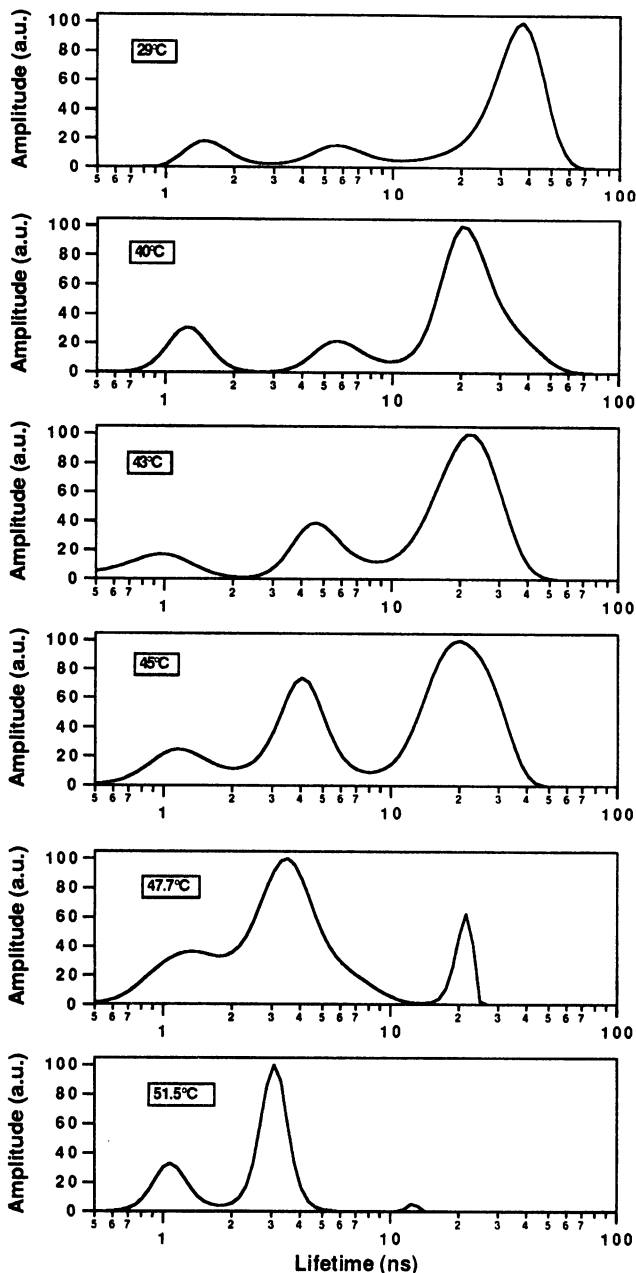


FIGURE 6 Effect of temperature on the lifetime distribution of *t*-PnA in large unilamellar vesicles of an equimolar mixture of DMPC/DPPC at 500 bar.

transition are smaller than those induced by temperature (Mateo et al., 1993a). For instance, at constant temperature, the *t*-PnA lifetimes in DMPC undergo a change from 4.2 to 17 ns, which is associated to the change in the lipid packing density. However, at constant pressure, the lifetime increases from 4.2 to 24 ns during the phase transition. In the latter case, the lifetime variation reflects not only the increase in the lipid packing density associated to the gel phase but also the temperature dependence of the *t*-PnA radiationless decay rate (Sklar et al., 1977).

The effect of pressure in lipid membranes have been described and studied in detail in saturated systems such as DMPC or DPPC but not as yet in unsaturated lipid bilayers.

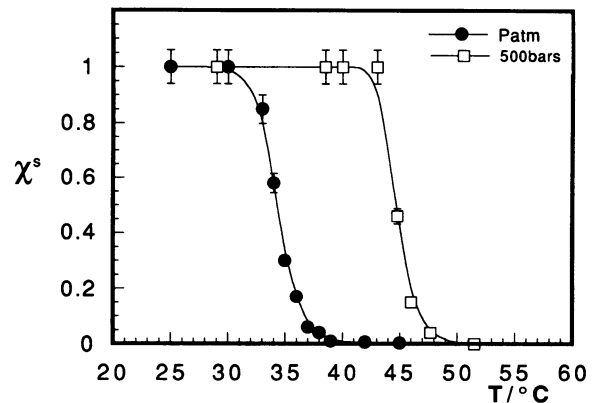


FIGURE 7 Temperature dependence of the gel phase fraction  $\chi^S$  of large unilamellar vesicles of an equimolar mixture of DMPC/DPPC at 1atm (●) and at 500bar (□).

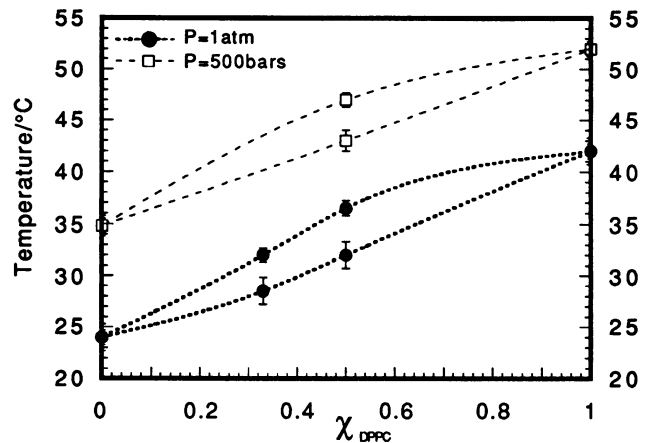


FIGURE 8 Effect of pressure on the thermotropic phase diagram of the DMPC/DPPC lipid mixture. (●) Phase diagram constructed at atmospheric pressure from the lifetime distributions of *t*-PnA (see preceding paper). (□) Data obtained at 500 bar (see text). At  $\chi_{DPPC} = 1$  and  $P = 500$  bar the temperature value is taken from Chong and Weber, 1983b.

Chong and Weber (1983b) examined by steady-state polarization fluorimetry of DPH the effect of pressure in lipid bilayers of dioleoylphosphatidylcholine (DOPC, one double *cis* bond in each chain) which presents a transition temperature at  $T_T = -20^\circ\text{C}$ . No isothermal pressure-induced transition was directly observed in this study since the upper limit of the pressure range was 2000 bar. However, they were able to estimate a  $dT/dP$  of  $21^\circ\text{C kbar}^{-1}$ . On the other hand, Siminovitch et al. (1987), studied by high pressure infrared spectroscopy the effect of pressure, up to 32 kbar, in DOPC bilayers and they determined a value for  $dT/dP \leq 8.3^\circ\text{C kbar}^{-1}$ . POPC (only one *cis* double bond on the *sn*-2 chain) is a not very studied unsaturated phospholipid which is an important component of animal cell membranes. In a recent paper (Sassaroli et al., 1993) the intramolecular excimer formation rate for dipy<sub>10</sub>PC was used to determine the effect of pressure in multilamellar vesicles of POPC. For this system the authors estimated a temperature to pressure equivalence  $dT/dP$  of  $19^\circ\text{C kbar}^{-1}$ . As this intramolecular excimer for-

**TABLE 4** Parameter values resulting from analysis of the anisotropy decay of DPH in DMPC

$P$	$\beta_1$	$\theta_1$	$\beta_2$	$\theta_2$	$r_\infty$	$r(0)$	$D_w$	$\eta$	$\langle P_2 \rangle$
bars		ns		ns			ns <sup>-1</sup>	poise	
1	0.167	0.7	0.127	1.9	0.026	0.320	0.134	0.31	0.26
100	0.162	1.2	0.099	3.1	0.056	0.317	0.103	0.46	0.38
300	0.104	0.3	0.146	2.3	0.136	0.386	0.079	0.53	0.59
600	0.040	0.3	0.022	2.2	0.275	0.337	0.062	0.67	0.84

$\beta_i$  and  $\theta_i$  are, respectively, the integrated amplitude and center value of each rotational correlation time component.  $\langle P_2 \rangle$ ,  $D_w$ , and  $\eta$  are determined from Eqs. 5–7 (see text).  $\beta_i$ ,  $\pm 0.008$ ;  $\theta_i$ ,  $\pm 0.3$  ns;  $r_\infty$ ,  $\pm 0.008$ .

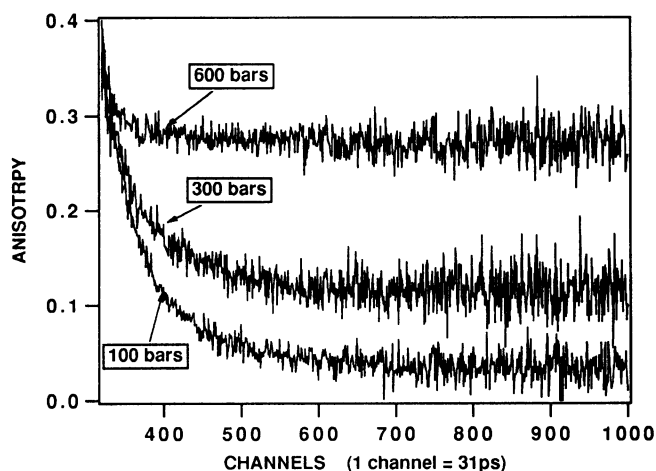


**FIGURE 9** Effect of pressure on the fluorescence anisotropy decay of DPH in large unilamellar vesicles of DMPC at 35°C.

mation rate was not very sensitive to the POPC isothermal phase transition, the accuracy of  $dT/dP$  determination is limited. With *t*-PnA, the POPC isothermal phase transition is marked by an abrupt drop in the gel phase fraction. This sharp drop allows to estimate with high precision a temperature to pressure equivalence of  $14.5^\circ\text{C kbar}^{-1}$ . This value is intermediate between that observed for saturated systems and the value determined for DOPC by Siminovitch et al. (1987). These authors concluded that either  $dT/dP$  is pressure-dependent, or the value of  $dT/dP$  is anomalously low. We find that the latter conclusion is more likely to be corrected and we think that  $dT/dP$  is dependent of the number and type of unsaturations of the phospholipids.

The molar volume increase  $\Delta V$  associated with the phase transition at atmospheric pressure can be evaluated from the Clausius-Clapeyron equation ( $dT/dP = T_m \Delta V/\Delta H$ ). The enthalpy of the phase transitions,  $\Delta H$ , for DMPC and POPC are 5.4 (Mabrey and Sturtevant, 1976) and 8.0 kcal/mol, respectively (Nagle and Wilkinson, 1978). Using our values of  $dT/dP$ , we have obtained a volume increase  $\Delta V = 18$  ml/mol for both DMPC and POPC. For DMPC, the change is in agreement with the value determined from density measurements (Nagle and Wilkinson, 1978).

The lipid components in many biological membranes appear to be organized in domains even at physiological temperatures. Alteration of pressure will lead to changes in the structure and size of domains and, probably, in the functional state on the membrane. Our results show that relatively mod-

erates pressures of about 500 bar shift  $11.5^\circ\text{C}$  the region of coexistence of the gel and fluid phases in DMPC/DPPC mixtures. This result indicates the extreme sensitivity to pressure of the organization of the different lipid environments.

Time-resolved fluorescence anisotropy experiments of DPH indicate that hydrostatic pressure increases both lipid orientational order and membrane viscosity. The equivalences between temperature and pressure  $dT/dP$  determined here are based on the comparison of the effects of temperature and pressure on the lipid phase transition. In principle, such experiments are not able to inform if the same equivalence can be applied to the molecular order and local viscosity. Assuming that this equivalence is the same, the pressure effect on the order parameter and rotational diffusion coefficient of DPH in DMPC (Table 4) was transformed in temperature effect using  $dT/dP = 24^\circ\text{C kbar}^{-1}$  (Fig. 11). The data agree well with those determined at different temperatures by Ameloot et al. (1984), indicating that the assumed equivalence is more or less correct. This is valid, at least, in the range of the pressure and temperature studied. From these results we can conclude that, although the pressure dependence of DPH location in the bilayer is not known, the probe can detect with precision the lipid phase transition induced by pressure and gives relative information about the changes produced in the order and fluidity of the pressurized membranes.

The fluorescent fatty acid *t*-PnA appears to be a good probe in the detection of membrane lateral heterogeneity and in the determination of the lipid orientational order. However, it is not very useful in detecting alterations in the membrane fluidity. Unlike DPH, *t*-PnA is not a rigid molecule and can present different molecular motions which are beyond our present experimental accuracy (Mateo et al., 1993a). However, the high sensitivity of its fluorescence kinetics to the physical state of the bilayer allows us to resolve the structural properties of different lipid environments and then to determine the effect of pressure on these environments. This is illustrated in Fig. 12. At constant temperature, an increase of pressure in the region of coexistence of the fluid and gel phases, decreases the fraction of fluid phase but makes it much more ordered. Simultaneously, the fraction of gel phase increases, but the molecular order of the corresponding lipid domains remains constant. The progressive ordering effect in the fluid phase as increasing pressure is presumably due to the reduction of volume of the bilayer itself and to the progressive packing by the lipid bulk, i.e., gel phase domains.

**TABLE 5** Fluorescence anisotropy decay parameters of *t*-PnA in LUVs of POPC and DMPC/DPPC equimolar mixtures calculated according to the associative model

System	<i>T</i>	<i>P</i>	$\theta_f$	$r_\infty^F$	$\theta_s$	$r_\infty^S$	$\langle P_2 \rangle^F$	$\langle P_2 \rangle^S$	<i>r</i> (0)	
	°C	bar	ns		ns					
	10	1	1.9	0.138			0.595		0.279	
		500	2.3	0.122			0.560		0.267	
		700	3.8	0.120		0.5	0.189	0.555	0.696	0.265
		900	4.9	0.156		0.2	0.243	0.632	0.789	0.237
		1100	0.2	0.171		0.2	0.198	0.662	0.713	0.400
		1400				<0.1	0.227		0.763	0.238
		2000				<0.1	0.218		0.748	0.239
POPC	20	1	1.5	0.071			0.426		0.279	
		500	2.4	0.086			0.469		0.230	
		900	1.6	0.134			0.586		0.230	
		1100	2.7	0.140		0.4	0.163	0.599	0.646	0.250
		1400	0.2	0.167		0.7	0.222	0.654	0.754	0.283
		1800	0.2	0.162		1.4	0.229	0.644	0.766	0.265
		2400				<0.1	0.200		0.716	0.249
DMPC/DPPC	38	1	0.8	0.104		0.294	0.516	0.868	0.279	
		150	0.6	0.141		0.2	0.293	0.601	0.867	0.301
		300	0.2	0.220		0.1	0.294	0.751	0.868	0.400
		500				<0.1	0.282		0.850	0.400

$\langle P_2 \rangle^F$  and  $\langle P_2 \rangle^S$  are, respectively, the order parameters of the probe in the fluid and gel phases.  $\theta_i$ ,  $\pm 0.3$  ns;  $r_\infty$ ,  $\pm 0.005$ .

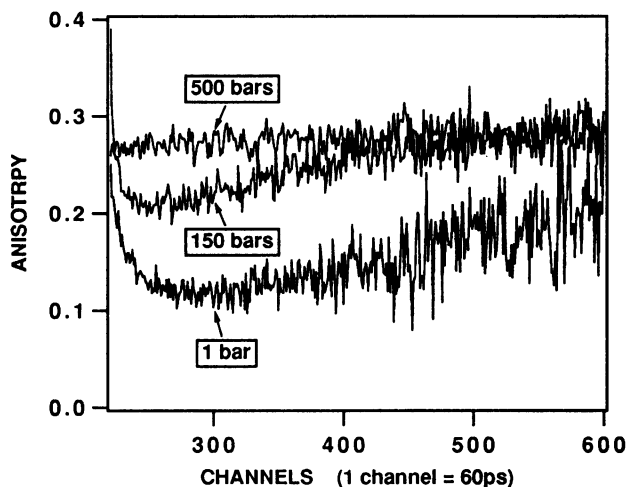


FIGURE 10 Effect of pressure on the fluorescence anisotropy decay of *t*-PnA in large unilamellar vesicles of an equimolar mixture of DPPC/DMPC at 38°C.

The effect of pressure on the molecular order of the fluid phase is similar to that induced by a temperature decrease (Mateo et al., 1993a). However, in the gel phase this effect is different: the change induced by temperature in the  $\langle P_2 \rangle^S$  value, from 0.82 to 0.95 (Mateo et al., 1993a), cannot be produced with pressure. At 38°C the order parameter was only  $0.86 \pm 0.01$ , at all the pressures studied. This indicates that, at this temperature, the thermal energy of the system hinders a higher lipid packing.

Unlike DMPC/DPPC, the anisotropy decay of *t*-PnA in POPC at the transition pressure can be relatively well fitted using a single population model. However, a double population model gave a better fit. Since the fluorescence lifetime distribution profiles indicates the coexistence of gel/fluid phase, we can conclude that a double population model reflects more the reality. The absence of the upward curvature

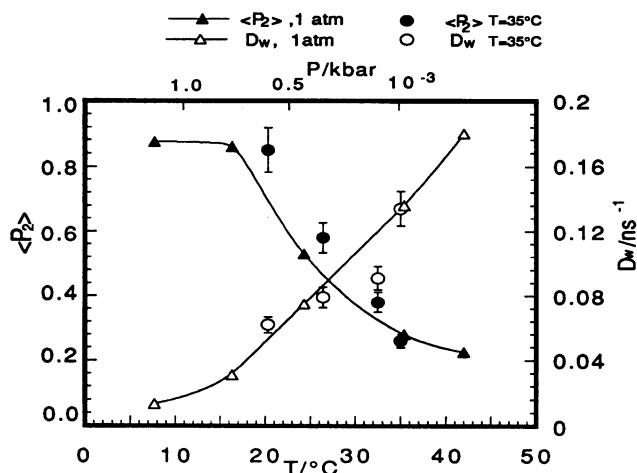


FIGURE 11 Effect of pressure, transformed in equivalent temperature by  $dT/dP = 24^\circ\text{C kbar}^{-1}$ , on the order parameter (●) and rotational diffusion coefficient (○) of DPH in DMPC. Data are compared with the values of  $\langle P_2 \rangle$  (▲) and  $D_w$  (△) obtained in a similar system at atmospheric pressure and as a function of temperature from Ameloot et al. (1984).

in the anisotropy decay is simply explained from the combination of the numerical values of lifetimes and anisotropy parameters (Brochon et al., 1992; Ludescher et al., 1987). The upward curvature arises when the fluorescence associated to the fluid system decays very fast, such that, at longer times the only contribution to the anisotropy signal corresponds to the probe in the more ordered system. However, if the fluorescence in the fluid system decays rather slowly and more or less simultaneously to that corresponding to the ordered system (in other words, if the respective lifetimes are not largely different) then the resulting total anisotropy decays smoothly. This is clearly illustrated in our data. In the case of DPPC/DMPC mixtures at 38°C and  $P = 150$  bar, the long fluorescence lifetimes in the fluid and gel phase are 4.7

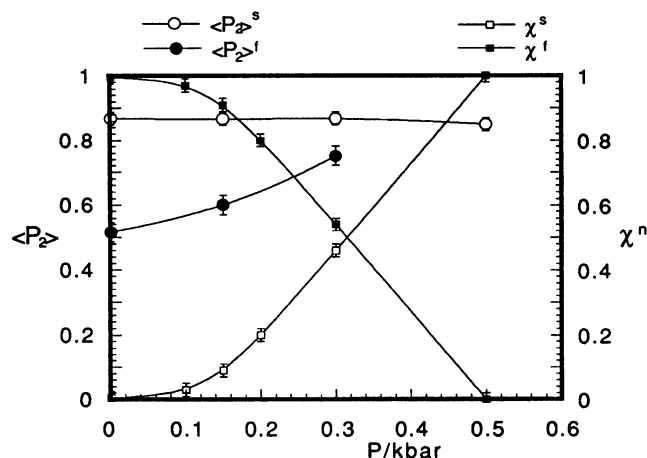


FIGURE 12 Effect of pressure on the fraction of fluid (■) and gel phase (□) of DMPC/PPC and the associated order parameters  $\langle P_2 \rangle^f$  (●) and  $\langle P_2 \rangle^s$  (○) at 38°C.

and 25 ns, respectively (see Table 1), which means a relative lifetime change of 5.3. However, in POPC vesicles at 10°C and at the phase transition pressure, the lifetimes associated to each phase are 12 and 34 ns, respectively, which is a factor of increase of only 2.8. On the other hand, the residual anisotropy in the gel and fluid phases of the lipid mixture are 0.29 and 0.14, respectively, whereas in POPC these are only 0.24 and 0.16. The simulation of an anisotropy decay using the above mentioned values gives for the lipid mixture and POPC vesicles the anisotropy curves showed in Fig. 13. In the curve corresponding to the lipid mixture the large difference between the lifetimes of the solid and fluid species causes the more ordered environment with its longer lifetime and higher anisotropy to dominate the decay at long times. This results in the observed upward curvature. In contrast, because of the smaller change in the lifetimes, the curve corresponding to POPC does not present upward curvature, and it could also be simulated assuming a single population of fluorophores with  $r_\infty = 0.225$ .

The difference observed between the order parameters of the gel phase in a bilayer of saturated phospholipids, DMPC and DMPC/DDPC, and in POPC indicates that the POPC lipids remain more disordered. This result is logical in considering the structure of this unsaturated phospholipid, where an acyl chain coexists with a *cis* double bond together with the other saturated chain. An efficient packing of the hydrocarbon chains could be hindered by steric interactions.

In conclusion, our results show that hydrostatic pressure affects, at least, three properties of the lipid bilayers: orientational order, membrane viscosity, and lateral heterogeneity. The equivalence between the effect of temperature and hydrostatic pressure on these structural properties,  $dT/dP$ , is dependent on the nature of phospholipid in the bilayer. Changes in orientational order and membrane viscosity are detected from the fluorescence anisotropy of DPH. The change in the gel-fluid heterogeneity is well detected from the fluorescence lifetime distribution of *t*-PnA. Similar pressure effects could be observed in the lateral heterogeneity of

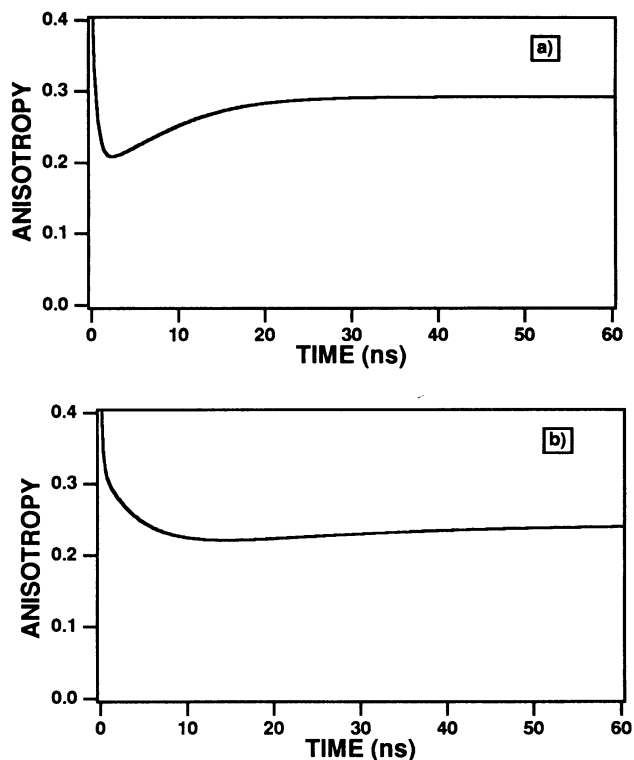


FIGURE 13 Simulated anisotropy decays calculated according to Eq. 3: (Curve a) with  $a_F = 0.67$ ,  $\tau_F = 4.7$  ns,  $\theta_F = 0.6$  ns,  $r_\infty^f = 0.141$ ,  $a_S = 0.33$ ,  $\tau_S = 25$  ns,  $\theta_S = 0.2$  ns, and  $r_\infty^s = 0.292$ . (Curve b) with  $a_F = 0.48$ ,  $\tau_F = 12$  ns,  $\theta_F = 5$  ns,  $r_\infty^f = 0.156$ ,  $a_S = 0.52$ ,  $\tau_S = 34$  ns,  $\theta_S = 0.2$  ns, and  $r_\infty^s = 0.243$ .  $r(0)$  was 0.4 in both curves.

more complex membrane systems. Relatively low pressures can alter the local fraction and composition of the lateral domains which have important biochemical implications. Further measurements of time-resolved fluorescence of *t*-PnA in pressurized phospholipid/cholesterol and lipid/protein bilayers could bring more insight on these systems.

We thank Dr. Ulises Acuña for many helpful discussions and for comments on the manuscript. We also thank Dr. I.Moya of LURE for use of his picosecond laser. The technical staff of LURE are acknowledged for running the synchrotron machine during the beam session. We also acknowledge financial support from an EC-LURE grant. C. R. Mateo acknowledges the support of a fellowship from the Consejo Superior de Investigaciones Científicas.

A summary of this work has been presented at a recent symposium (Tauc et al., 1993).

## REFERENCES

- Ameloot, M., H. Hendrickx, W. Herreman, H. Pottel, F. Van Cauwelaert, and W. van der Meer. 1984. Effect of orientational order in the decay of the fluorescence anisotropy in membrane suspension. *Biophys. J.* 46: 525-539.
- Behan, M. K., A. G. Macdonald, G. R. Jones, and A. R. Cossins. 1992. Homeoviscous adaptation under pressure: the pressure dependence of membrane order in brain myelin membranes of deep-sea fish. *Biochim. Biophys. Acta.* 1103:317-323.
- Best, J., E. John, and F. Jähnig. 1987. Order and fluidity of lipid membranes as determined by fluorescence anisotropy decay. *Eur. Biophys. J.* 15:87-102.

- Braganza, L. F., and D. L. Worcester. 1986a. Hydrostatic pressure induced hydrocarbon chain interdigitation in single-component phospholipid bilayers. *Biochemistry*. 25:2591-2596.
- Braganza, L. F., and D. L. Worcester. 1986b. Structural changes in lipid bilayers and biological membranes caused by hydrostatic pressure. *Biochemistry*. 25:7484-7488.
- Brochon, J. C., and A. K. Livesey. 1988. Time-resolved fluorimetry using synchrotron radiation and maximum entropy method of analysis. In *Light in Biology and Medicine*. R. H. Douglas, J. Moan, and F. Dall'Acqua, editors. Plenum Publishing Corp. New York. 21-29.
- Brochon, J. C., F. Merola, and A. K. Livesey. 1992. Time-resolved fluorescence study of dynamics parameters in biosystem. In *Synchrotron Radiation and Dynamic Phenomena*. Vol. 258. American Institute of Physics, New York. 435-452.
- Ceuterick, F., J. Peeters, K. Heremans, H. de Smedt, and H. Olbrechts. 1978. Effect of high pressure, detergents and phospholipase on the break in the arrhenius plot of azotobacter nitrogenase. *Eur. J. Biochem.* 87:401-407.
- Chong, P. L.-G., A. R. Cossins, and G. Weber. 1983a. A differential polarized phase fluorometric study of the effects of high hydrostatic pressure upon the fluidity of cellular membranes. *Biochemistry*. 22:409-415.
- Chong, P. L.-G., and G. Weber. 1983b. Pressure dependence of 1:6-diphenyl-1,3,5-hexatriene fluorescence in single-component phosphatidylcholine liposomes. *Biochemistry*. 22:5544-5550.
- Chong, P. L.-G., B. W. van der Meer, and T. E. Thompson. 1985. The effects of pressure and cholesterol on rotational motions of perylene in lipid bilayers. *Biochim. Biophys. Acta.* 813:253-265.
- Chong, P. L.-G. 1988. Effects of hydrostatic pressure on the location of PRODAN in lipid bilayers and cellular membranes. *Biochemistry*. 27:399-404.
- Heyn, M. P. 1989. Order and viscosity of membranes: analysis by time-resolved fluorescence depolarization. *Methods. Enzymol.* 172:462-471.
- Hope, M. J., M. B. Bally, G. Webb, and P. R. Cullis. 1985. Production of large unilamellar vesicles by a rapid extrusion procedure. Characterisation of size distribution, trapped volume and ability to maintain a membrane potential. *Biochim. Biophys. Acta.* 812:55-65.
- Hudson, B. S., D. L. Harris, R. D. Ludescher, A. Ruggiero, A. Cooney-Freed, and S. A. Cavalier. 1986. Fluorescence probe studies of protein and membranes. In *Applications of Fluorescence in the Biomedical Sciences*. D. L. Taylor, A. S. Waggoner, F. Lanni, R. F. Murphy, and R. Birge, editors. Alan R. Liss, Inc., New York. 159-202.
- Hudson, B. S., and S. A. Cavalier. 1988. Studies of membrane dynamics and lipid-protein interactions with parinaric acid. In *Spectroscopic Membrane Probes*, Vol. 1. L. M. Loew, editor. CRC Press, Inc., Boca Raton. FL. 43-62.
- Jähnig, F. 1979. Structural order of lipids and proteins in membranes: evaluation of fluorescence anisotropy data. *Proc. Natl. Acad. Sci. USA.* 76:6361-6365.
- Jonas, J., C.-L. Xie, A. Jonas, P. J. Grandinetti, D. Campbell, and D. Driscoll. 1988. High-resolution <sup>13</sup>C NMR study of pressure effects on the main phase transition in L- $\alpha$ -dipalmitoyl phosphatidylcholine vesicles. *Proc. Acad. Sci. USA.* 85:4115-4117.
- Jones, G. R., and R. B. Cunadall. 1986. The effect of moderately high pressure on the fluorescence spectra of 1:6-diphenylhexatriene, 1,6-[4,4'-dicyanophenyl]hexatriene and 1,8-diphenyloctatetraene. *Chem. Phys. Lett.* 126:129-133.
- Kinosita, K., S. Kawato, and A. Ikegami. 1977. A theory of fluorescence polarisation decay in membranes. *Biophys. J.* 20:289-305.
- Kinosita, K., S. Kawato, and A. Ikegami. 1984. Dynamic structure of biological and model membranes: analysis by optical anisotropy decay measurement. *Adv. Biophys.* 17:147-203.
- Liu, N.-I., and R. L. Kay. 1977. Redetermination of the pressure dependence of the lipid bilayer phase transition. *Biochemistry*. 16:3484-3486.
- Ludescher, R. D., L. Peting, S. Hudson, and B. Hudson. 1987. Time-resolved fluorescence anisotropy for systems with lifetime and dynamic heterogeneity. *Biophys. Chem.* 28:59-75.
- Mabrey, S., and J. M. Sturtevant. 1976. Investigation of phase transitions of lipids mixtures by high sensitivity differential scanning calorimetry. *Proc. Natl. Acad. Sci. USA.* 73:3862-3866.
- Macdonald, A. G. 1983. The hyperbaric liposome. In *Liposome Letters*. Academic Press, London. 231-249.
- Mateo, C. R., J. C. Brochon, M. P. Lillo, and A. U. Acuña. 1993a. Lipid bilayer lateral clustering as detected by the fluorescence kinetics and anisotropy of trans-parinaric. *Biophys. J.* 65:2237-2247.
- Mateo, C. R., M. P. Lillo, J. C. Brochon, M. Martinez, J. Sainz, and A. U. Acuña. 1993b. Rotational dynamics of 1:6-diphenyl-1,3,5-hexatriene and derivatives from fluorescence depolarization. *J. Phys. Chem.* 97:3486-3491.
- Moya, I., M. Hodges, and J.-C. Barbet. 1986. Modification of room-temperature picosecond chlorophyll fluorescence kinetics in green algae by photosystem II trap closure. *FEBS Lett.* 198:256-262.
- Nagle, J. F., and D. A. Wilkinson. 1978. Lecithin bilayers. Density measurements and molecular interactions. *Biophys. J.* 23:159-175.
- Paladini, A., and G. Weber. 1981. Absolute measurements of fluorescence polarization at high pressures. *Rev. Sci. Instrum.* 52:419-427.
- Peng, X., and J. Jonas. 1992. High-pressure <sup>31</sup>P NMR study of dipalmitoylphosphatidylcholine bilayers. *Biochemistry*. 31:6383-6390.
- Sassaroli, M., P. Vauhkonen, P. Somerharju, and S. Scarlata. 1993. Dipyrrenylphosphatidylcholines as membrane fluidity probes: pressure and temperature dependence of the intramolecular excimer formation rate. *Biophys. J.* 64:137-149.
- Siminovitch, D. J., P. T. T. Wong, and H. H. Mantsch. 1987. Effects of cis and trans unsaturation on the structure of phospholipid bilayers: a high-pressure infrared spectroscopic study. *Biochemistry*. 26:3277-3287.
- Sklar, L. A., B. S. Hudson, M. Petersen, and J. Diamond. 1977. Conjugated Polyene fatty acids on fluorescent probes: spectroscopic characterisation. *Biochemistry*. 16:813-818.
- Tauc, P., C. R. Mateo, and J. C. Brochon. 1993. Effects of hydrostatic pressure on the structure of phospholipid bilayers as detected by the fluorescence kinetics of trans-parinaric acid. *Biophys. J.* 64:243a. (Abstr.)
- Tosh, R. E., and P. J. Collings. 1986. High pressure volumetric measurements in dipalmitoylphosphatidylcholine bilayers. *Biochim. Biophys. Acta.* 850:10-14.
- Trudell, J. R., D. G. Payan, J. H. Chin, and N. Cohen. 1974. Pressure-induced elevation of phase transition temperature in dipalmitoylphosphatidylcholine bilayers: an electron spin resonance measurement of the enthalpy of phase transition. *Biochim. Biophys. Acta.* 373:436-443.